1985

Semiclassical Calculation of Quantum-Mechanical Wave Functions for a Two-Dimensional Scattering System

Stephen Knudson
William & Mary

John B. Delos
William & Mary, jbdelo@wm.edu

B. Bloom
William & Mary

Recommended Citation

Knudson, Stephen; Delos, John B.; and Bloom, B., Semiclassical Calculation of Quantum-Mechanical Wave Functions for a Two-Dimensional Scattering System (1985). *Journal of Chemical Physics*, 83(11), 5703-5711.
https://doi.org/10.1063/1.449645

Semiclassical calculation of quantum-mechanical wave functions for a two-dimensional scattering system

S. K. Knudson, J. B. Delos, and B. Bloom
Departments of Chemistry and Physics, College of William and Mary, Williamsburg, Virginia 23185

(Received 1 March 1985; accepted 19 August 1985)

The semiclassical theory developed by Maslov and Fedoriuk is used to calculate the wave function for two-dimensional scattering from a Morse potential. The characteristic function S and the density Jacobian J are computed in order to obtain the primitive wave function. The incident part shows distorted plane-wave behavior and the scattered part shows radially outgoing behavior. A uniform approximation gives a wave function that is well behaved near the caustic.

I. INTRODUCTION

For more than a century, the semiclassical or JWKB approximation has been one of the standard methods for constructing solutions of one-dimensional differential equations. There has long been a need for the development of a corresponding method for solving differential equations in two or three dimensions. Elastic, inelastic, and reactive scattering of atoms from molecules are examples of processes which can be described by solving an n-dimensional Schrödinger equation, and for which semiclassical approximations are known to be appropriate. It is not surprising, therefore, that important contributions to this mathematical problem have been made by molecular physicists and theoretical chemists.[1] On the other hand, it is also not surprising that some of the most fundamental mathematical questions were not addressed in that work.

A careful and thorough mathematical exposition of n-dimensional semiclassical theory has recently been given by Maslov and Fedoriuk (MF),[2] and a simplified summary of the essential concepts that they developed will soon be published.[3] Part of the purpose of the present work is to close the gap between abstract mathematical theorems and useful computational methods. As suggested above, these two facets of semiclassical theory have developed somewhat independently of each other. On one hand, while MF have developed the theory in great detail, they have not, to our knowledge, ever actually used their ideas to compute a nontrivial wave function. On the other hand, much of the ongoing calculational work cited in Ref. 1 would profit from an appreciation of the mathematical advances presented in MF.

In the present paper, the theory created by Maslov and Fedoriuk is used for the first time to calculate a wave function for a very simple system—elastic scattering of a particle on a Morse potential in two dimensions.

Semiclassical scattering amplitudes and differential cross sections for elastic scattering are already understood through the work of Ford and Wheeler and others[4] many years ago. Methods similar to theirs (partial wave expansion, one-dimensional WKB approximation, and stationary phase summation) could also be used to obtain the wave function, but apparently no one has ever carried out such a calculation. For this purpose, the methods developed by MF are quite appropriate, easily providing the wave function everywhere, and (if desired) scattering amplitudes and differential cross sections as well. Furthermore, in contrast to methods based upon partial-wave expansions, the present methods are very easily extended to systems that do not have spherical symmetry. Finally, the Morse scattering system provides particulary clear and simple illustrations of many of the abstract concepts discussed in Refs. 2 and 3.

II. SUMMARY OF THE PROCEDURE FOR CALCULATION OF WAVE FUNCTIONS

MF's mathematical theorems implicitly specify a constructive procedure for calculation of wave functions, and we state the rules of this procedure as concisely as possible in this section. Subsequently, in Secs. III–VI, the procedure is carried out to obtain a wave function (a more complete discussion of the procedure is given in Ref. 3, and of course the full treatment, together with all proofs, is presented by MF[2]).

We wish to obtain a semiclassical approximation for the wave function $\Psi(q)$, which is a solution to the Schrödinger equation

$$\left[H\left(-i\hbar\frac{\partial}{\partial q}, q\right) - E\right]\Psi(q) = 0 \tag{2.1}$$

a linear partial differential equation in n variables $(q_1 \ldots q_n)$, collectively denoted q (configuration space). Associated with the Hamiltonian operator $H(-i\hbar\partial/\partial q, q)$ is the Hamiltonian function $H(p,q)$ defined in the $2n$-dimensional phase space $(p, q) = (p_1 \ldots p_n, q_1 \ldots q_n)$. A formal asymptotic approximation to $\Psi(q)$ is constructed by the following steps:

(i) Compute trajectories. A family of trajectories is calculated by integration of Hamilton's equations from specified initial conditions. The rules for allowable initial conditions are a bit complicated. (a) One chooses an $(n-1)$-dimensional initial surface in the n-dimensional configuration space; coordinates spanning this initial manifold are denoted $w^0 = \{w_i^0 | i = 1 \ldots n-1\}$, and the embedding of the initial manifold in configuration space is given by n smooth functions $\{q_i^0(w^0) | i = 1 \ldots n\}$. (b) For each point q^0, an initial momentum $p^0(q^0)$ and an initial value of a characteristic function $S^0(q^0)$ are specified, subject to certain restrictions. First, $p^0(q^0)$ must satisfy

$$H[\mathrm{BK}: p^0(q^0), q^0] = E. \tag{2.2}$$

 0021-9606/85/235703-09$02.10

Second, $S^0(q^0)$ must be such that for any increment dq^0 restricted to the initial surface

$$dS^0 = p^0(q^0)\cdot dq^0 = \sum_{i=1}^{n} p_i^0(q^0)dq_i^0. \tag{2.3}$$

Subject to these restrictions, the initial conditions are mathematically arbitrary, and they are chosen in accordance with the physical boundary conditions imposed on the wave function. From those initial conditions, an $(n-1)$-parameter family of trajectories, and the characteristic function S for this family, is calculated by integration of Hamilton's equations

$$\dot{p}_i = -\partial H/\partial q_i, \tag{2.4a}$$

$$\dot{q}_i = \partial H/\partial p_i, \tag{2.4b}$$

$$\dot{S} = p\cdot\dot{q} = \sum_{i=1}^{n} p_i dq_i/dt. \tag{2.4c}$$

This integration generates (pointwise) a set of $2n+1$ functions of n variables

$$q_i = q_i(t, w^0), \tag{2.5a}$$

$$p_i = p_i(t, w^0), \tag{2.5b}$$

$$S = S(t, w^0). \tag{2.5c}$$

(ii) Represent trajectories as a manifold in phase space, and select charts. The functions $[p(t, w^0), q(t, w^0)]$ correspond to an n-dimensional surface in the $2n$-dimensional phase space, and this surface is called a Lagrangian manifold. The manifold can be spanned by the n "intrinsic" coordinates (t, w^0)—time and the $n-1$ coordinates spanning the initial manifold. This manifold must now be divided into overlapping domains ("charts"), each of which makes use of a set of n phase-space coordinates that is appropriate for that domain. A domain is said to be *regular* if it has a smooth and smoothly invertible ("diffeomorphic") projection into part of configuration space. For such a domain the functions $\{q_i(t, w^0)|i = 1...n\}$ obtained by integration of Eq. (2.4) are smooth, and the relationship between (t, w^0) and q is one to one and smoothly invertible. It follows that in a regular domain, configuration space coordinates can be regarded as the independent variables, and the embedding of the manifold in phase space can be described by n smooth functions $p(q) = \{p_i(q_1...q_n)|i = 1...n\}$. (These functions need not actually be constructed, but the picture that they provide of the topological structure of the manifold is needed.)

Domains that are not regular are called singular. For each singular domain, one must select a set of n phase-space coordinates $(p_\alpha, q_\beta) = \{p_i|i\in\alpha\} \otimes \{q_j|j\in\beta\}$, where α and β are disjoint sets containing, respectively, k and n-k elements. This means that the set $p_\alpha q_\beta$ contains no canonically conjugate pairs. (Such a set $\{p_\alpha q_\beta\}$ is called a "Lagrangian coordinate plane.") This set is chosen in such a way that the manifold has a diffeomorphic projection into a portion of the $p_\alpha q_\beta$ plane. Then the embedding of this domain of the manifold in phase-space is given by n functions $(p_\beta, q_\alpha) = \{p_j(p_\alpha q_\beta)|j\in\beta\} \otimes \{q_i(p_\alpha q_\beta)|i\in\alpha\}$. MF have proved that stable singular domains always admit such a representation.

On the manifold one must also define a set of "switching functions," or a "partition of unity": a set of positive functions $e_j(t, w^0)$ such that

$$\sum_j e_j(t, w^0) = 1 \tag{2.6}$$

and such that each e_j is nonzero only in the jth domain, where it is close to unity. These switching functions are used to join different locally valid asymptotic approximations into one smooth global wave function.

(iii) Calculate generator and Jacobian in each regular chart. Integration of Eqs. (2.4) also generates the quantity S, which is single valued and smooth on the manifold and which may be represented by a function $S(t, w^0)$. Within any regular domain, since there is a smooth and smoothly invertible relationship between configuration-space points q and manifold points (t, w^0), we may alternatively regard this same quantity S as a function of q. Using notation that is conventional in physics, we shall always denote the characteristic function as S regardless of what the independent variables are, and write in the jth regular domain

$$S \equiv S(t, w^0) = S_j(q). \tag{2.7}$$

$S(q)$ is also called the generator for the specified domain of the manifold and it will be seen to become part of the phase of the wave function.

Also, in each regular domain, a Jacobian

$$J = \partial(q)/\partial(t, w^0) \tag{2.8}$$

must be computed and represented as a function of q. Because there is an invertible relationship between q and (t, w^0), this Jacobian is finite and nonzero in the regular domain. The Jacobian determines the amplitude of the wave function.

The representation of S and J as functions of q involves the inversion of the relationship $q(t, w^0)$ that is obtained from integration of Eq. (2.4). That integration gives positions q as functions of (t, w^0); to calculate $S(q)$ and $J(q)$, one might specify q, compute the corresponding value of (t, w^0) (the intrinsic coordinates for the manifold), and then find the associated values of S and J. An interpolation procedure may be used to carry this out.

(iv) Calculate the Maslov index μ_j for each regular domain. The Maslov index μ_j for the jth regular chart is calculated using the prescription given in Ref. 3 (there are some errors in Ref. 2). One regular chart is selected as the initial chart, and μ for that chart is (arbitrarily) set to zero. A curve is defined that goes from any arbitrary initial point in the initial chart to an arbitrary final point in the jth chart. The curve is divided into sections, and the total value of μ_j is the sum of the values obtained for each section. For each section that lies entirely in a regular chart, the contribution to μ_j is zero. For each section that lies in a singular chart having coordinates $(p_\alpha q_\beta)$, the contribution is

$$\text{inerdex}\left(\frac{\partial q_\alpha}{\partial p_\alpha}\right)_{\text{initial}} - \text{inerdex}\left(\frac{\partial q_\alpha}{\partial p_\alpha}\right)_{\text{final}}, \tag{2.9}$$

where the inerdex of a matrix is the number of negative eigenvalues of the matrix. The inerdex is evaluated at the initial and final points of each section of the curve, with the entire section lying within one chart.

The Maslov index can often be obtained simply by inspection of the topological structure of the manifold.

(v) Calculate generator and Jacobian for each singular chart. The characteristic function $S(t, w^0)$ is well defined, single valued, and smooth over the entire manifold. In each singular domain, having already chosen a suitable mixed set of coordinates for the domain, the generator

$$\tilde{S} = S - p_\alpha q_\alpha = S - \sum_{i \in \alpha} p_i q_i \tag{2.10}$$

is calculated, as is the corresponding Jacobian

$$\tilde{J} = \partial(p_\alpha, q_\beta)/\partial(t, w^0)\,. \tag{2.11}$$

Both of these quantities have to be regarded as functions of $p_\alpha q_\beta$. [This again requires the inversion of the computed relationship $(tw^0) \rightarrow (p_\alpha q_\beta)$.]

(vi) Calculate the index ν_j for each singular chart. The index ν_j (not to be confused with μ_j) is also defined in Ref. 3. To calculate it one defines a chain or sequence of overlapping charts, of which the first is the initial chart and the last is the singular chart of interest. At each place in the chain where we switch from one chart to another, there is a contribution to ν_j of

$$\text{inerdex}\left(\frac{\partial q_\alpha}{\partial p_\alpha}\right)_{\text{final}} - \text{inerdex}\left(\frac{\partial q_\alpha}{\partial p_\alpha}\right)_{\text{initial}}\,. \tag{2.12}$$

Here the inerdex is evaluated for two different charts at the same point on the manifold. The index ν_j is the sum of such contributions, one from each change of charts in the chain.

(vii) Calculate contributions to $\Psi(q)$ from each chart, and sum. At each configuration point q, the domains of the Lagrangian manifold that project to q must be identified. Each such regular domain contributes

$$\Psi_j(q) = |\rho^0[w^0(q)]|^{1/2}\,|J_j(q)|^{-1/2}\,e_j(q) \times \exp\{i[S_j(q)/\hbar - \tfrac{1}{2}\mu_j\pi]\}, \tag{2.13}$$

where $S_j(q)$, $J_j(q)$, and μ_j are the characteristic function, Jacobian, and Maslov index for the jth regular domain. The quantity $\rho^0(w^0)$ is an initial density associated with the field of trajectories; in the cases of immediate interest it is a smooth, but otherwise mathematically arbitrary function of w^0, defined on the initial manifold in accordance with the physical boundary conditions on the wave function.

Each singular chart having coordinates $(p_\alpha q_\beta)$ gives a wave function in the corresponding mixed space of coordinates and momenta that is equal to

$$\tilde{\Psi}_j(p_\alpha q_\beta) = |\rho^0[w^0(p_\alpha q_\beta)]|^{1/2}\,|\tilde{J}_j(p_\alpha q_\beta)|^{-1/2}\,e_j\,p_\alpha q_\beta \times \exp\{i[\tilde{S}_j(p_\alpha q_\beta) - \tfrac{1}{2}\nu_k\pi]\}. \tag{2.14}$$

The associated contribution to the configuration-space wave function is the Fourier transform of $\tilde{\Psi}_j$:

$$\Psi_j(q) = (-2\pi i\hbar)^{-k/2} \int \exp(ip_\alpha q_\alpha/\hbar) \times \tilde{\Psi}_j(p_\alpha q_\beta) e_j(p_\alpha q_\beta)\, dp_\alpha\,. \tag{2.15}$$

As mentioned earlier, k is the number of variables in the set α and e_j is the switching function attached to the jth chart.

In applications of Eqs. (2.14) and (2.15), one may make use of simplifying approximations. For example, a suitably chosen Taylor expansion of $\tilde{S}$ and $\tilde{J}$ leads in the simplest cases to Airy-function approximations.

Finally, the full wave function is given by a sum of contributions from each chart.

$$\Psi(q) = \sum_j \Psi_j(q). \tag{2.16}$$

The relative amplitudes and phases of the terms in this sum are all implicitly included in the formulas given above.

III. TRAJECTORIES AND THE MANIFOLD

We now consider the scattering of a particle of mass M from a central potential $V(R)$. For a central potential the scattering occurs in a plane; we take it to be the XZ plane, with the origin of the coordinate system at the scattering center and the initial direction of motion of the particle taken to be Z. In order to eliminate additional interference effects, we limit impact parameters to positive X, making this a restricted two-dimensional problem. We also employ polar coordinates

$$R = (X^2 + Z^2)^{1/2}, \quad \Theta = \tan^{-1}(X/Z)\,, \tag{3.1}$$

so that R is the radial distance from the scattering center to the particle and the angle Θ is measured in the counterclockwise sense from the forward (positive Z) axis. We use a Morse potential

$$V(R) = D\exp[-a(R - R_e)] \times \{\exp[-a(R - R_e)] - 2\} \tag{3.2}$$

with potential parameters $a = 2.5$, $D = 1$ eV, and $R_e = 2^{1/6}$ in atomic units except as noted. The Hamiltonian is then

$$H = (P_x^2 + P_z^2)/2M + V(R), \tag{3.3}$$

where the P's are the canonical momenta. The classical Hamiltonian equations of motion are then explicitly, in polar coordinates,

$$\begin{aligned} &dR/dt = P_R/M, \quad d\Theta/dt = -L/MR^2, \\ &dP_R/dt = L^2/MR^3 + 2aD\exp[-a(R - R_e)] \times \{\exp[-a(R - R_e)] - 1\}, \\ &dL/dt = 0. \end{aligned} \tag{3.4}$$

The energy E and the angular momentum $L = (2ME)^{1/2}b$ are both constants of motion; conservation of energy is used only as a check on the numerical accuracy of the integration, but conservation of angular momentum is used to reduce the number of trajectory equations integrated to the first three in Eq. (2.4). The energy[5] is taken to be $E = 1.6$ (eV) and the reduced mass $M = 1$. The trajectory starts at time $t = 0$ from $Z = Z^0$, where $|Z^0|$ is large, with an impact parameter $b = X^0$. The initial momentum is in the $+Z$ direction with magnitude $(2ME)^{1/2}$. As discussed above, these conditions correspond to a one-dimensional Lagrangian manifold spanned by the coordinate $w^0 \equiv b \equiv X^0$, and condition (2.2) is satisfied. Integration of trajectories then gives a two-dimensional Lagrangian manifold in the four-dimensional phase space. Any point on a trajectory can be characterized by its impact parameter b and the time t. The final direction of a trajectory is called the scattering angle, designated Θ_F.

Solution of Eqs. (2.4) for a number of different impact

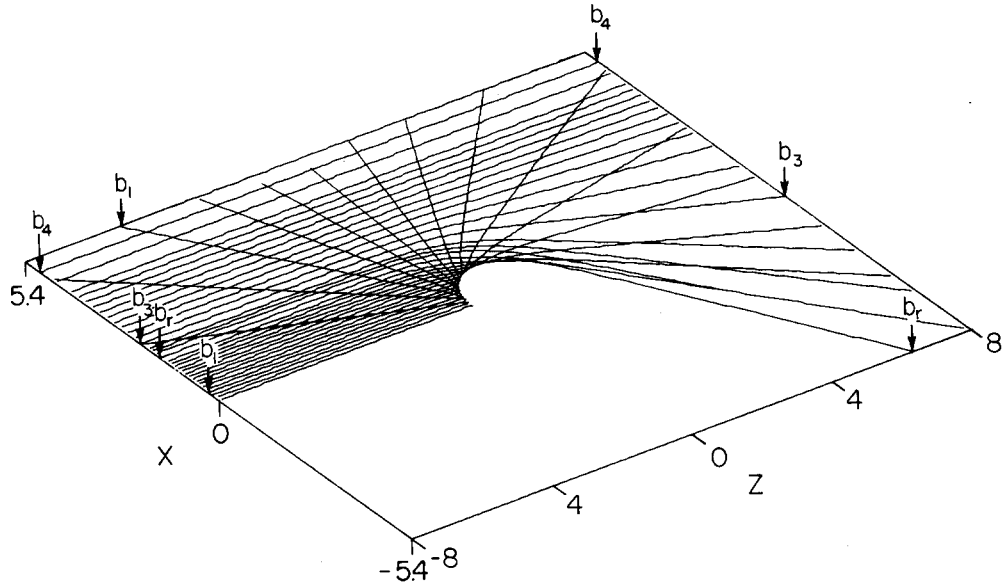

FIG. 1. The family of trajectories for two-dimensional scattering from a Morse potential. Each trajectory begins at $Z = -8$ with various values of $X^0 = b$. The region devoid of trajectories is the classically forbidden region, separated from the allowed region by the caustic. The labeled impact parameters b_j denote the beginning and the end of representative trajectories.

parameters generates the field of trajectories displayed in Fig. 1 (in a perspective consistent with that of later figures displaying S, J, and Ψ). For trajectories starting at large impact parameter b such as the trajectory labeled b_4, the influence of the potential is very weak; the trajectory is therefore essentially a straight line, with the scattering angle Θ_F very small and negative. As the impact parameter decreases a trajectory such as b_3 feels the attractive part of the potential, and scatters to negative Θ_F. As b continues to decrease and the repulsive forces grow, the scattering angle attains a minimum value, called the rainbow angle Θ_r, on the trajectory having impact parameter $b = b_r$. Trajectories starting at very small b, e.g., b_1, are strongly repelled by the inner portion of the potential, and scatter out to large positive angles.

The curve which separates the classically allowed from the classically forbidden portion of configuration space is the caustic; it is made up of the locus of points at which adjacent trajectories cross over each other. As seen in Fig. 1, for the Morse potential the caustic is roughly circular at small Z, and it becomes nearly linear for large Z.

An approximate representation of the manifold is shown in Fig. 2. We partition this manifold into four overlapping charts, each with a particular domain.

I (incident): the portion of the manifold representing tra-

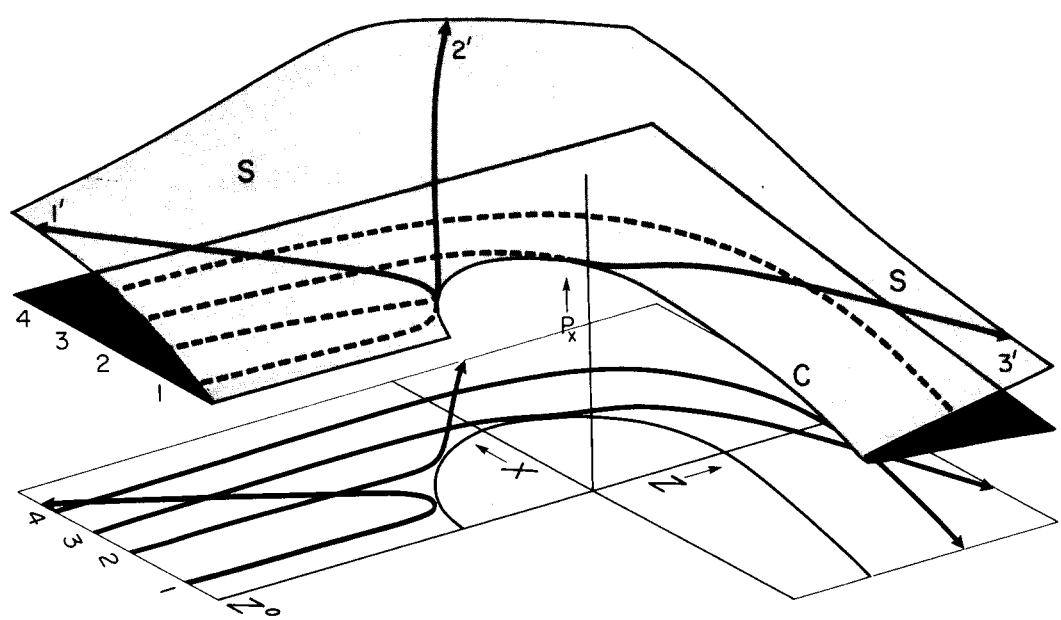

FIG. 2. Qualitative picture of the Lagrangian manifold for a typical family of elastically scattered trajectories. The manifold is represented as a two-dimensional surface in the reduced phase space (XZP_X). The lower sheet of the manifold contains trajectories which have not touched the caustic; the upper sheet contains trajectories that have passed through the caustic. Labeled trajectories help to define the shape of the surface. The trajectory labeled (1 — 1') begins with $P_X^0 = 0$, X^0 small, and $Z = Z^0$. On the incoming part of this trajectory, while Z decreases, X remains nearly constant, and P_X remains small. As the trajectory passes through the caustic, P_X increases rather suddenly, then becomes approximately constant on the outgoing part of the trajectory. The trajectory labeled (3 — 3') also begins with $P_X^0 = 0$, $Z = Z^0$, but with larger X^0. This trajectory mainly feels the attractive part of the potential energy and P_X decreases as t increases. After the trajectory passes through the caustic, P_X approaches a negative constant. The trajectory (4 — 4') never passes through the caustic, but otherwise is quite similar to (3 — 3').

jectories or parts of trajectories that have not touched (and may never touch) the caustic. Trajectories having $b > b_r$ generally lie entirely within the I domain, so much of I corresponds to nearly rectilinear trajectories; however, I also include trajectories that have been pulled by the attractive force into the region $X < 0$.

S (scattered): the portion of the manifold representing parts of trajectories that have glanced off the caustic. This domain includes only the later (large t) portions of trajectories having $b < b_r$. Both I and S are restricted to be "not too close" to the caustic.

C (caustic): The portions of the manifold that are close to the caustic. This is divided further into C_1, corresponding to the "semicircular" part of the caustic, and C_2, the "linear" part.

Domains I and S are regular and configuration coordinates (X,Z) are appropriate. Domains C_1 and C_2 are singular.

For singular domains of the manifold, any Lagrangian coordinate plane (p_α, q_β) can be used, provided that the domain has a smooth projection into that plane [MF have proved an important theorem which asserts that (to order $\hbar$) the wave function is invariant under changes of Lagrangian coordinates]. Most of C_1 has a smooth projection into the (Z, P_X) plane and therefore those coordinates could be used in that region. Even better are the coordinates (Θ, P_R)—the polar angle and the radial momentum, since these coordinates are nearly parallel to and perpendicular to the caustic. To obtain a similar Lagrangian coordinate plane for the C_2 domain, we define rotated Cartesian coordinates

$$U = Z\cos\Theta_r - X\sin\Theta_r,$$

$$V = -Z\sin\Theta_r - X\cos\Theta_r$$

such that U and V run, respectively, parallel to and perpendicular to the linear part of the caustic. It follows that the pair (U, P_V) are appropriate coordinates for this domain.

We shall also define the "I sheet" of the manifold to include the I domain and the "precaustic" part of the C domains, and the "S sheet" to include the S domain and the "post-caustic" part of the C domains. For the remainder of the paper we will use a subscript I (or S) to denote quantities associated with incident (or scattered) sheets. For this scattering problem, one incident and one scattered trajectory pass through each point in the accessible portion of the XZ plane.

In order to obtain the results of the trajectory integrations in the form required for plotting, a two-dimensional (X,Z) grid is established in the scattering plane, spaced at 0.1 a.u. increments in both directions. Each time a trajectory passes through any of the Z-grid lines, the sheet and the values of X, of P_X, and of the functions S and J described in the next section are stored. Data from many trajectories with different impact parameters are used to provide these values over the entire plane for both incident and scattered classes. On each Z-grid line this information is then interpolated to give values at the X-grid intersections; this interpolation must be done separately for the incident and scattered sheets of the manifold. Trajectory data at the caustic is also stored and interpolated along the caustic as required to obtain the uniform wave function below.

IV. THE CHARACTERISTIC FUNCTION S, THE JACOBIAN J, AND THE MASLOV INDEX

In order to determine the semiclassical wave function, we need to compute two functions, the characteristic function $S(X,Z)$ and the Jacobian $J(X,Z)$. We first consider S, which is a solution of the Hamilton–Jacobi equation

$$H\left(\frac{\partial S}{\partial X}, \frac{\partial S}{\partial Z}, X, Z\right) = \frac{1}{2M}|\nabla S|^2 + V(X,Z) = E \tag{4.1}$$

and which is calculated by integrating Eq. (2.5c)

$$S(X,Z) = S^0(X^0, Z^0) + \int\left(P_X\frac{dX}{dt} + P_Z\frac{dZ}{dt}\right)dt \tag{4.2}$$

along the trajectory connecting the initial point X^0Z^0 with XZ. As explained in Refs. 2 and 3, if the integral (4.2) is to satisfy the Hamilton–Jacobi equation (4.1), the initial values $S^0(X^0, Z^0)$ must be chosen in an appropriate manner. From Eq. (2.3) we see that for the scattering problem, S^0 must be constant along the initial surface $Z = Z^0$, and the nearby lines of constant S then represent plane waves incident on the target. One sees from Fig. 2 that locally [for short times in Eq. (3.2)] $S(X,Z)$ is unique, but globally S is a two-valued function of position, one value being associated with each sheet of the manifold $S_I(X,Z)$ and $S_S(X,Z)$. Each of these functions is single valued and continuous up to the caustic, where the two functions join each other continuously.

The surfaces S_I and S_S are shown in Figs. 3(a) and 3(b), respectively, and below each surface members of the appropriate trajectory class are inscribed. The behavior of S_I and S_S is easy to understand when one remembers that $\mathbf{P} = \nabla S$; the incident surface S_I begins at $Z = Z^0$ with the (arbitrary) initial value of zero and for large X^0 (large impact parameter), S_I increases linearly with increasing Z, consistent with the nearly rectilinear trajectories in this region. Above the caustic, S_I increases in the direction of motion of the trajectories, which is along the caustic. The surface S_I is joined to S_S at the caustic and S_S generally increases radially with increasing R, corresponding to the outward motion of the scattered trajectories.

The Jacobian is given by Eq. (2.8),

$$J = \partial(q)/\partial(t, w^0) = \partial(Z,X)/\partial(t,b) = \frac{\partial X}{\partial b}\frac{dZ}{dt} - \frac{dX}{dt}\frac{\partial Z}{\partial b} \tag{4.3}$$

and it can be expressed in polar coordinates as

$$J = -R\left[\left(\frac{\partial R}{\partial b}\right)\frac{d\Theta}{dt} - \frac{dR}{dt}\frac{\partial\Theta}{\partial b}\right]. \tag{4.4}$$

The velocities in this formula can be obtained directly from the data for a single trajectory, but the derivatives with respect to impact parameter b cannot. In order to obtain these $\partial/\partial b$ terms, pairs of trajectories at adjacent impact parameters $b + \Delta b/2$ and $b - \Delta b/2$ are in fact used. The numerical derivatives, e.g., $\{Z(t, b + \Delta b/2) - Z(t, b - \Delta b/2)\}/\Delta b$, are found to be stable for Δb between 0.01 and 0.000 001 a.u.; we used $\Delta b = 0.0003$ a.u. The Jacobian is computed as the trajectories are integrated. It is also single valued on the manifold, but two valued in configuration space.

The Jacobian is plotted in Fig. 4. From Eq. (4.3), the initial value of J is $(2E/M)^{1/2}$ and J stays close to this asymptotic value over most of the incident portion of the manifold.

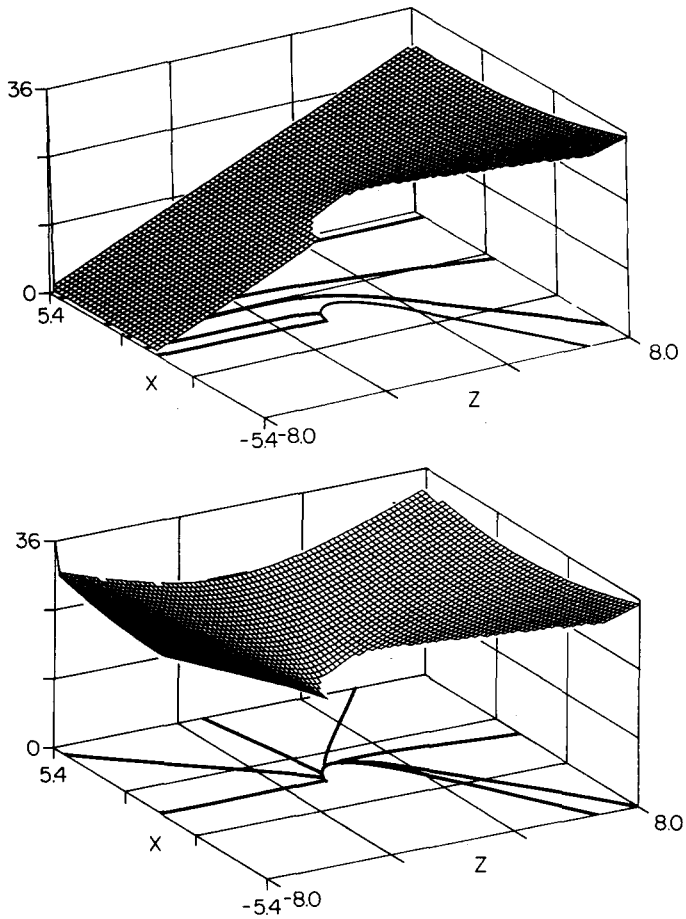

FIG. 3. (a) The characteristic function S_I of Eq. (4.2). Members of the incident class of trajectories and the caustic are inscribed below the surface. Note that the scale is not square. (b) The characteristic functions S_S of Eq. (4.2). Members of the scattered class of trajectories and the caustic are inscribed below the surface. Note that the scale is not square.

On the part corresponding to scattered trajectories, the first term in Eq. (4.4) becomes small and J is approximately $(2E/M)^{1/2} R (\partial\Theta/\partial b)$, so its magnitude increases linearly with R. The classical density is therefore inversely proportional to R in this region, as one would expect for radially outgoing trajectories.

To calculate the Maslov indices, we follow the instructions given in Sec. V C of Ref. 3 and stated more briefly earlier in this paper. To calculate, consider any curve $l[w^0, w]$ on the manifold that starts from any point w^0 on the initial surface and ends at an arbitrary point w. If the curve lies entirely within the I chart, because that chart is regular, $\mu(l) = 0$. If the curve enters the chart C, this chart has coordinates (Θ, P_R) and the relevant matrix in Eq. (2.9) is $(\partial R/\partial P_R)_\Theta$. Within C_1, this derivative has the same properties as $(\partial X/\partial P_X)_Z$, the behavior of which is easily seen from the qualitative sketch of the manifold (Fig. 2). Near the caustic, on the I sheet, it is negative, while on the S sheet it is positive. Therefore, inerdex $(\partial X/\partial P_X)$ is $+1$ (one negative eigenvalue) for points in C_1 on the I sheet, and 0 (no negative eigenvalues) for points in C_1 on the S sheet. Hence, a curve in C_1 that goes from the I sheet to the S sheet has an index $\mu =$ (initial inerdex–final inerdex) $= 1$. Finally, since for any curve that lies *entirely* within the S sheet $\mu(l) = 0$, it follows that any curve having initial point on the incident sheet and final point on the scattered sheet has $\mu(l) = 1$.

The index of such curves gives the Maslov index of the regular domains, so we have $\mu_I = 0, \mu_S = 1$.

Similar but appropriately modified reasoning is used to calculate the index ν, which is defined by the properties of a chain of charts. Each sequence or chain begins with the chart I for which the set p_α is empty and inerdex $(\partial q_\alpha/\partial p_\alpha) = 0$. For the sequence $[I - C_1]$, we switch from coordinates XZ to coordinates $(P_X Z)$ somewhere on the I sheet, where $\partial X/\partial P_X < 0$ and its inerdex is $+1$. Therefore, according to Eq. (2.12), the index ν associated with this sequence is $1 - 0 = 1$. In contrast to μ, ν does not change within chart C_1. For the sequence $[I - C_1 - S]$, ν has a contribution of 1 from the sequence $[I - C_1]$ and we need to find the contribution from the $[C_1 - S]$ part. In the upper part of C_1, we already stated that $\partial X/\partial P_X > 0$ and inerdex $= 0$, and in S the set P_α is again empty, so its inerdex is also zero, and from Eq. (2.12) the contribution of $[C_1 - S]$ to ν is zero.

The index ν_{C_1} for chart C_1 is just equal to ν for the sequence $[I - C_1]$, so it is also equal to unity. The same is true for chart C_2.

These quantities can now be used to determine semiclassical wave functions. We first discuss the primitive semiclassical wave function.

V. PRIMITIVE WAVE FUNCTION

The formula for an individual term in the primitive function is given by Eq. (2.14). For the case of two-dimensional potential scattering, the initial density $\rho^0(w^0)$ is a constant (the flux density of the incident beam is independent of impact parameter) so this equation takes the form

$$\Psi(X, Z) = |J(X, Z)|^{-1/2} \exp[iS(X, Z)/\hbar - i\mu\pi/2]. \quad (5.1)$$

There is one term of this type for each of the charts I and S. Surfaces of constant phase of these functions are lines of constant S_I or S_S and these are indicated in Fig. 5. The lines

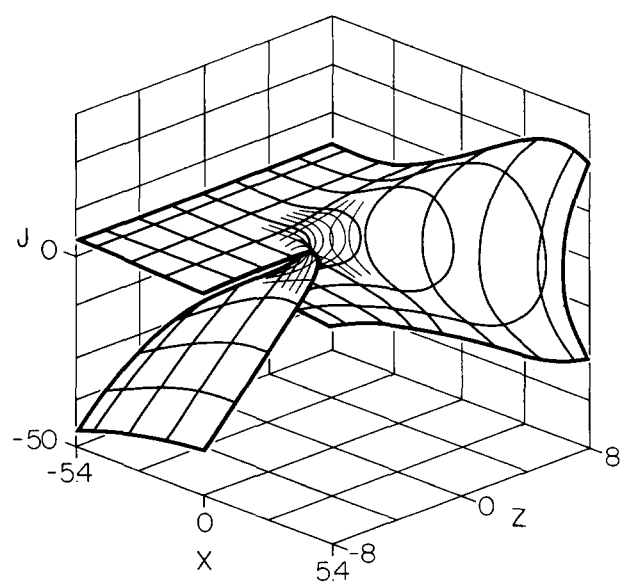

FIG. 4. The Jacobian manifold J [Eq. (4.3)]. The upper sheet is J_I, the lower J_S.

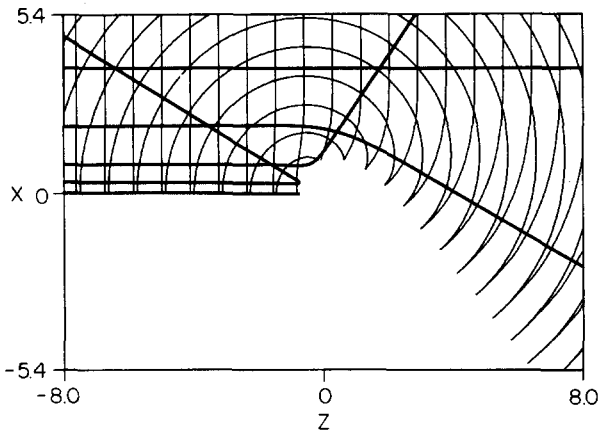

FIG. 5. Contour plots of S_I and S_S with selected trajectories. The contours are the wavefronts for which the trajectories are the "rays." Contour lines are located at integer multiples of $\pi/2$.

of constant S_I are initially straight, corresponding to the incoming plane wave motion. There are small deviations near the caustic, where the potential is important, and refraction around the scattering center is also evident.

One is tempted to describe the surfaces of constant S_S as "outgoing circular wavefronts," but Fig. 5 shows that the word "circular" should not be taken too literally. The wavefronts are not really circular nor even elliptical. In the usual description of wave scattering, the boundary conditions involve outgoing circular (or spherical) waves at large distances, and the asymptotic form the wave function is written as

$$f(\Theta)e^{ikR}/R^{1/2}. \tag{5.2}$$

The exponential factor in Eq. (5.2) does describe circular waves, but the preexponential factor is complex, and to compare Eq. (5.2) with Eq. (5.1), we would have to recognize that

$$S_S(R,\Theta)/\hbar - \mu\tfrac{1}{2}\pi + i\ \ln[J_S(R,\Theta)/2] \overset{R\to\infty}{\to} kR - i\ \ln[f(\Theta)/R^{1/2}] + \text{constant}. \tag{5.3}$$

Thus the phase effects described by noncircular scattered waves in the present approach are contained in the phase of the scattering amplitude $f(\Theta)$ in the conventional approach.

Surfaces of constant S_S join the surfaces of constant S_I in a cusp-like manner at the caustic. This means that if the Maslov indices μ for both charts were equal, then crests and troughs of the incident waves would meet crests and troughs of the scattered waves at the caustic. In fact, however, since $\mu = 1$ in the S chart, but $\mu = 0$ in the I chart, it follows that (e.g., in the real part of Ψ) a crest of incident waves meets a node of scattered waves, and an incident node meets a scattered trough.[6] [Alternatively, if the time dependent factor $\exp(-iEt/\hbar)$ were included in the wave function, we could say that the scattered wave is "delayed" 1/4 wavelength behind the incident wave.]

The imaginary part of Ψ_I and the real part of Ψ_S are shown in Fig. 6. Both of these functions are expected to be reasonably accurate everywhere except near the caustic, where J vanishes; there the singularity in both wave functions is apparent. Note that this unphysical behavior in the primitive wave function is confined to a narrow region im-

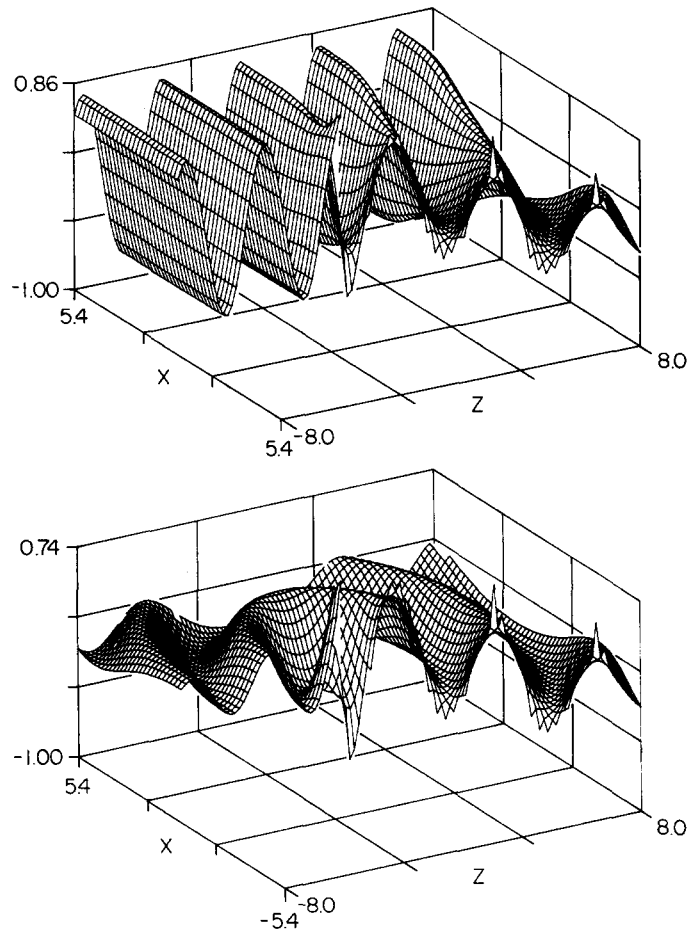

FIG. 6. (a) The imaginary part of the primitive incident semiclassical wave function [Eq. (5.1)]. (b) The real part of the primitive scattered semiclassical wave function [Eq. (5.1)].

mediately adjacent to the caustic.

The incident primitive function displays the plane-wave oscillatory motion expected from the character of the wavefronts of S_I. The oscillations are modified in the region $Z>0$, $X<0$, which in Fig. 6 is above and behind the linear portion of the caustic. Here the crests of the waves run at about a 45° angle to the original direction. This is related in the obvious way to the trajectories (Fig. 5) and it can also be understood from a different point of view.

Hamilton's analogy between rays of geometrical optics and trajectories of classical dynamics tells us that the index of refraction $n(q)$ in an inhomogeneous medium corresponds to the classical quantity $[E - V(q)]^{1/2}$ times a constant. Therefore, the attractive well of the potential energy produces an effect that is similar to that of a medium with a large index of refraction. Plane waves entering the region refract and bend around the target. The potential energy therefore acts as a lens, which produces outgoing refracted waves in the region $X<0, Z>0$. The amplitude of these refracted rays is proportional to $R^{-1/2}$, consistent with the behavior of the Jacobian in Fig. 4.

The scattered wave function Ψ_S shows curved outgoing waves with amplitude again proportional to $R^{-1/2}$.

The total primitive semiclassical wave function is given by the sum of the incident and scattered terms at each point.

$$\Psi_P(X,Z) = |J_I(X,Z)|^{-1/2}\exp[iS_I(X,Z)/\hbar] + |J_S(X,Z)|^{-1/2}\exp[iS_S(X,Z)/\hbar - \tfrac{1}{2}\pi]. \tag{5.4}$$

We defer discussion of this result until the uniform terms are included.

VI. UNIFORM WAVE FUNCTION

In the forbidden region and near the caustic, the primitive wave function is unsuitable and a better approximation is obtained by Fourier transformation of a momentum-space or mixed-space form. The formula we use here is sometimes called a "transitional approximation"—it gives a result that is adequate only in the vicinity of the caustic.

The singular part of the manifold was divided into two charts C_1 and C_2. In C_1, since the caustic is shaped more or less like a semicircle, polar coordinates provide a useful representation. Transformation into momentum space can be justified in polar as well as Cartesian coordinates, so we can write in domain C_1:

$$\Psi_{C_1} = (-2\pi i\hbar)^{-1/2} e^{-i\pi\nu_{C_1}/2}\int_{-\infty}^{\infty} e(P_R,\Theta)|\tilde{J}(P_R,\Theta)|^{-1/2} \times\exp\{i[P_R R + \tilde{S}(P_R,\Theta)]/\hbar\}\, dP_R. \tag{6.1}$$

Here $e(P_R,\Theta)$ is an appropriate switching function, which is equal to unity in chart C_1 and which goes to zero elsewhere, and ν_{C_1} is a Maslov index for the chain of charts $[I - C_1]$, which was shown to be equal to unity.

With further approximations, Eq. (6.1) can be converted to the Airy-function form given in Eq. (5.26) of Ref. 3. We define

$$\Phi(P_R; R, \Theta) = RP_R + \tilde{S}(P_R,\Theta) \tag{6.2}$$

and expand Φ in a Taylor series in P_R, using

$$\partial\Phi/\partial P_R = R + \partial\tilde{S}/\partial P_R = R - R(P_R,\Theta), \tag{6.3}$$

$$\partial^2\Phi/\partial P_R^2 = -\partial R(P_R,\Theta)/\partial P_R, \tag{6.4}$$

$$\partial^3\Phi/\partial P_R^3 = -\partial^2 R(P_R,\Theta)/\partial P_R^2. \tag{6.5}$$

Equations (6.3)–(6.5) use the same notation as does Ref. 3. R is one of the *independent variables* in Ψ, but $R(P_R,\Theta)$ is one of the *functions* defining the embedding of the manifold in phase space [i.e., one of the functions $q_\alpha(p_\alpha, q_\beta)$]. R and $R(P_R,\Theta)$ need not be equal to each other. With derivatives given above, we may Taylor-expand Φ about the point P_C such that

$$\partial R(P_R,\Theta)/\partial P_R|_{P_R=P_C} = 0. \tag{6.6}$$

P_C is then the value of P_R on the caustic at angle Θ and $R(P_C,\Theta) = R_C$, the radius of the caustic at Θ. With the additional approximations that $|J(P_R,\Theta)|^{-1/2}$ is nearly constant and that the switching function is unity over the significant range of the integral, we obtain the leading term in the asymptotic expansion of the wave function

$$\begin{aligned}\Psi_{C_1} &= (-2\pi i\hbar)^{-1/2} e^{-i\pi/2}|\tilde{J}(P_C,\Theta)|^{-1/2}\exp[i\Phi(P_C;R,\Theta)/\hbar] \\ &\quad\times\int_{-\infty}^{\infty}\exp\{(i/\hbar)[(P_R-P_C)(R-R_C) - (P_R-P_C)^3/3\beta(\Theta)^3]\}\, dP_R \\ &= e^{-i\pi/4}\hbar^{-1/6}|2\pi/\tilde{J}(P_C,\Theta)|^{1/2}\beta(\Theta)\exp[i\Phi(P_C;R,\Theta)/\hbar]\mathrm{Ai}[-\beta(\Theta)(R_C-R)/\hbar^{2/3}],\end{aligned} \tag{6.7}$$

where

$$\beta(\Theta) = \left(\frac{1}{2}\frac{\partial^2 R(P_R,\Theta)}{\partial P_R^2}\bigg|_{P_R=P_C}\right)^{-1/3} \tag{6.8}$$

and

$$\Phi(P_C;R,\Theta) = S(R_C,\Theta) + P_C(R-R_C).$$

The leading Airy function term requires numerical evaluation of the second derivative given in Eq. (6.8), and higher-order corrections to the wave function involve successively higher derivatives, which are not easy to obtain accurately. We obtained better results by choosing $\beta(\Theta)$ in such a way that the magnitude of the primitive wave function is equal to the magnitude of the uniform wave function (6.7) at a distance from the caustic where both forms are valid. For numerical convenience, the value of $\beta(\Theta)$ obtained in this pointwise fashion was replaced by the approximation

$$\beta(\Theta) = -1 + 1.285(\Theta - \tfrac{1}{2}\pi) - \tfrac{1}{32}(\Theta - \tfrac{1}{2}\pi)^2. \tag{6.9}$$

In chart C_2, the caustic is nearly linear and we have chosen to use as coordinates

$$U = (Z+X)/\sqrt{2}, \qquad V = (Z-X)/\sqrt{2}, \tag{6.10}$$

because U and V are roughly parallel and perpendicular to the caustic, respectively. The uniform approximant in C_2 has the same form as in Eq. (5.7) above, with U replacing Θ and V replacing R:

$$\begin{aligned}\Psi_{C_2} &= e^{-i\pi/4}\hbar^{-1/6}|2\pi/\tilde{J}(U,P_V)|^{1/2}\beta(U) \\ &\quad\times\exp\{i[S_C(U) + P_V^C(V-V_C)]/\hbar\} \\ &\quad\times\mathrm{Ai}\{-\beta(U)[V-V_C(U)]/\hbar^{2/3}\}.\end{aligned} \tag{6.11}$$

Again, the parameter β is obtained by using a fit to the values found by matching the magnitudes of the primitive and uniform terms, and we found a good fit using

$$\beta(U) = 1.95 - 0.27\,U. \tag{6.12}$$

A switching function is used to stitch the two different Airy approximations together at the boundary between C_1 and C_2 near the Z axis. A second switching function is then used to combine the Airy and primitive approximations. The formulas for the switching functions are

$$\begin{aligned} e_1 &= \tfrac{1}{2}\{1 - \tanh[2.5(U-1.25)]\}, \\ e_2 &= \tfrac{1}{2}\{1 - \tanh[4(V - V_c - 0.3)]\}, \quad U>1 \\ &= \tfrac{1}{2}\{1 - \tanh[4(R - R_C - 0.4)]\}, \quad U<1 \end{aligned} \tag{6.13}$$

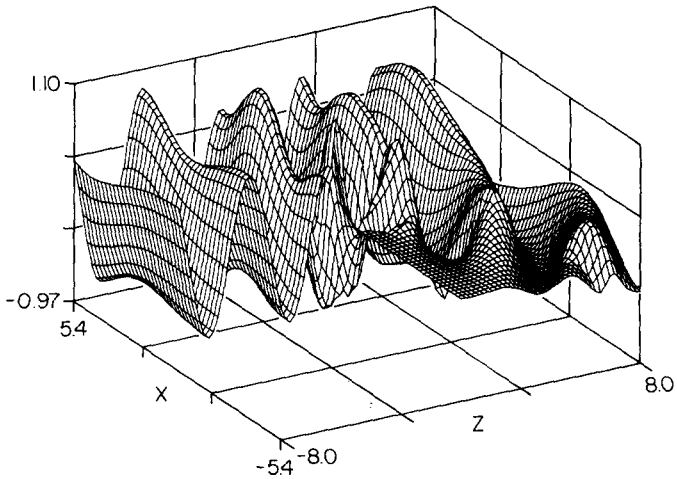

FIG. 7. Real part of the total semiclassical wave function for scattering from a Morse potential, obtained by combining the semiclassical wave function from each of the charts using switching functions [Eq. (6.14)].

and the final expression for the complete wave function is then

$$\Psi = \Psi_P(1 - e_2) + e_2[\Psi_{C_1} e_1 + \Psi_{C_2}(1 - e_1)]. \qquad (6.14)$$

The real part of the resulting wave function is shown in Fig. 7. The effect of the Airy terms is perhaps most clearly seen along the linear portion of the caustic. The decay of the wave function in the forbidden region is clearly depicted and the singularities in the primitive term are replaced by smooth maxima, as the primitive term joins onto the Airy function. It takes some effort to join the primitive and uniform wave functions smoothly and there is a bit of a bump in the wave function near the rightmost corner of the figure. This occurs primarily because the particular procedure used to determine the parameter β requires the magnitude of the wave function to be continuous; neither the real nor the imaginary part need separately be.

Away from the caustic the interference of the incident and scattered primitive terms is visible, most clearly at the larger X values near $Z = 0$. There the scattered term distorts the uniform oscillations of the incident wave, producing secondary maxima and minima.

Finally, let us mention again that for the present calculation we have included only the leading Airy function term, which is formally of order $\hbar^{-1/6}$. The next correction is of order $\hbar^{1/6}$ and it can easily be calculated using the method of Chester, Friedman, and Ursell[7] (see also Connor and Marcus[1(a)]). It gives an improved approximation near the caustic and the result also joins more smoothly onto the primitive semiclassical wave function.

VII. CONCLUSION

The mathematical developments made by Maslov and his co-workers are a major advance in semiclassical theory. Their formulation provides much-needed insight and deeper understanding of short-wavelength approximations for systems having several degrees of freedom.

In this paper, we have shown that the concepts they developed also lead to a simple and practical calculational method for obtaining wave functions. From such wave functions, all observable physical properties of a system can be found. We have illustrated the method by calculating $\Psi(q)$ for a simple and well-understood two-dimensional scattering system. In the future, we will examine the corresponding three-dimensional scattering system.

ACKNOWLEDGMENTS

The authors wish to acknowledge support for this research from the Jeffress Memorial Trust. JBD acknowledges support from the National Science Foundation and wishes to thank the J. Bruce Bredin Foundation for a research fellowship. Acknowledgment is made to the donors of the Petroleum Research Fund, administered by the ACS, for partial support of this research (SKK). We especially thank D. W. Noid for many helpful discussions.

[1]For example: (a) R. A. Marcus, Chem. Phys. Lett. **7**, 525 (1970); J. Chem. Phys. **54**, 3935 (1971); **56**, 311, 3548 (1972); Discuss. Faraday Soc. **55**, 34 (1973); J. N. L. Connor and R. A. Marcus, J. Chem. Phys. **55**, 5636 (1971); D. W. Noid and R. A. Marcus, *ibid.* **62**, 2119 (1975); (b) W. H. Miller, J. Chem. Phys. **53**, 1949, 3578 (1970); **54**, 5386 (1971); **57**, 2458 (1972). W. H. Miller and T. F. George, *ibid.* **56**, 5668 (1972); (c) J. B. Keller, Ann. Phys. **4**, 180 (1958); J. B. Keller and S. I. Rubinow, *ibid.* **9**, 24 (1960); D. J. Vezzetti and S. I. Rubinow, *ibid.* **35**, 373 (1965); (d) J. C. Y. Chen and K. M. Watson, Phys. Rev. **174**, 152 (1968); **188**, 236 (1969); J. C. Y. Chen, C.-S. Wang, and K. M. Watson, Phys. Rev. A **1**, 1150 (1970); (e) J. N. L. Connor, Mol. Phys. **31**, 33 (1976). Also **26**, 1217 (1973) and **27**, 853 (1974); (f) M. V. Berry, Adv. Phys. **25**, 1 (1976); (g) E. Heller, J. Chem. Phys. **62**, 1544 (1975); **75** 2923 (1981); M. J. Davis and E. Heller, *ibid.* **71**, 3383 (1979); **75**, 3916 (1981).

[2]V. P. Maslov and M. V. Fedoriuk, *Semiclassical Approximation in Quantum Mechanics* (Reidel, Boston, 1981).

[3]J. B. Delos, Adv. Chem. Phys. (in press).

[4]K. W. Ford and J. A. Wheeler, Adv. Phys. (NY) **7**, 259, 287 (1959); R. B. Bernstein, Adv. Chem. Phys. **10**, 75 (1966).

[5]The values of E and of the parameters in $V(R)$ are appropriate for typical low energy atom–atom collisions; however, for such situations the mass should be $> 2 \times 10^3$. The shapes of the classical trajectories in the center-of-mass frame are independent of the masses of the colliding particles, and therefore all of the classical quantities presented in this paper have realistic behavior. The wave function for a slow atomic collision also has a structure similar to what we show, but its oscillations would have a wavelength 30 or more times shorter than that indicated in our figures. Because of the difficulties of presenting graphs of such rapidly oscillating functions, we have taken the mass to be artificially small.

[6]Equivalently, since the wave function is complex, we can also say that crests in the *imaginary* part of Ψ_I meet crests in the *real* part of Ψ_S at the caustic, and likewise crests in the *real* part of Ψ_I meet crests in the *imaginary* part of Ψ_S at the caustic.

[7]C. Chester, B. Friedman, and F. Ursell, Proc. Cambridge Philos. Soc. **53**, 599 (1957).